Chapter 1

CLOSED LOOP IDENTIFICATION OF UNCERTAIN SYSTEMS

Magdi S. Mahmoud [†] and Haris M. Khalid[‡]

Abstract

Feedback is an important element in practical systems. However, it brings challenging situations in its route. In this paper, we deal with the closed-loop identification of a two-tank process used in industry. The identified model is then utilized to develop $\mathcal{H}_\infty$ and sliding mode controllers to develop robustness of the system. It is shown that these controllers guarantee a satisfactory performance in the face of both model/parametric uncertainties and external disturbances. The designed controllers have been successfully tested through extensive simulation. In addition, this paper shows that the designed linear and nonlinear robust controllers far outperform traditional controllers such as P, PI, and PID, in the face of parametric model uncertainties and the effects of external disturbances. The successful use of the designed robust controllers, which are $\mathcal{H}_\infty$, sliding-mode and high-order sliding mode controllers, encouraging their extension to other physical systems as well.

Keywords: closed loop identification, $\mathcal{H}_\infty$ control, sliding mode control, higher order sliding mode control, two-tank system.

Nomenclature

The variables used in the paper are expressed in Table 1.

1. Introduction

Modern closed loop identification has always been recognized as being one of the primary importance and has been the subject of intense research since the late sixties. It is widely

*Manuscript **MsM-KFUPM-Haris-CLI-Nova-Publishers.tex**

[†]M. S. Mahmoud is with the Systems Engineering Department, King Fahd University of Petroleum and Minerals, P. O. Box 985, Dhahran 31261, **Saudi Arabia** , e-mail: msmahmoud@kfupm.edu.sa.

[‡]H. M. Khalid is with the Systems Engineering Department, King Fahd University of Petroleum and Minerals, P. O. Box 8283, Dhahran 31261, **Saudi Arabia**, e-mail: mhariskh@kfupm.edu.sa

Table 1. Nomenclature

Symbol	Description
Q_i	Initial flow of water
Q_l	Increment in the nominal (leakage-free) of flow Q_l^0
Q_0	Output flow rate
$\varphi(u)$	Dead-band and saturation type of non-linearity
a_m	Motor system
b_m	Pump system
u	Input to the motor/Control Variable
Q_1	Leakage in Tank 1
C_0	Discharge coefficient of output valves
A_1	Cross-Sectional Area of Tank1
A_2	Cross-Sectional Area of Tank2
H_1	Height of Tank1
H_2	Height of Tank2
g	Gravitational constant
h_1	Increment in the nominal (leakage-free) of height H_1^0
h_2	Increment in the nominal (leakage-free) of height H_2^0
q_0	Increment in Q_0
q_i	Increment in Q_i
q_l	Increment in Q_l
k_p	Proportional gain in PI Controller
k_i	Integral gain in PI Controller
α	Associated with the leakage $q_1 = \alpha h_1$
β	Associated with the leakage $q_0 = \beta h_2$
nk	Different delays
v	Measured variable
w	Exogenous inputs, such as disturbances and commands
z	Exogenous outputs
S_o	Output sensitivity function
T	Complementary sensitivity function
$W_s()$	Weighting functions for sensitivity function
$W_u()$	Weighting functions for Complementary sensitivity function

recognized that in a large number of practical situations, feedback cannot be removed for various reasons including the following situations:

• Feedback may be intrinsic in the physical mechanism generating the data, or

• Data may come from an industrial plant where feedback loops cannot be opened due to safety or production quality reasons, or

• The physical mechanism might be too complex and may not be easily manipulated (for example a communication network)

Another reason for performing identification in a closed loop setting comes from the need to design experiments that would reduce the uncertainty in certain key frequency bands, to a desired level. Employing closed-loop in process control has numerous drawbacks, notably, the absence of a quality-check in the midst of the process, which results in a faulty output. For example, in a plant that mass-produces television sets, the process involves assembling CRTs and television bodies. During this assembly, if a body or a CRT gets damaged in the process, or even if it were damaged beforehand, a faulty product will be produced and the loop will be mistakenly acknowledged as having produced an acceptable product and will be allowed to continue to do so, until a subsequent quality-control stage detects the faulty products and alerts the operators that a remedial action is required. Identification of systems operating in a closed loop has received considerable attention in the system identification literature [1], [2], [3], [4], [5], [6]. There are safety and economic reasons for performing identification experiments in a closed loop setting. Also, it is known that the optimal experiment is usually performed in closed-loop [7], [8], [9], [6], [10]. Indeed, recent research has established that, for a general class of systems, and when there is a constraint on the output power, the optimal experiment is necessarily closed loop [11], [12]-[14].

Unfortunately, the identification of systems operating under the presence of feedback presents several difficulties [1], [6]. For example, correlation between the input signal and the noise is problematic in the context of several identification techniques. In fact, it is well known that the prediction error method provides a non-consistent estimate in the presence of under-modeling of the noise transfer function [1]. In [15], the effects of sampling time are investigated from both a theoretical and practical perspective using results that come out of the theory of closed-loop system identification with routine operating data.

Several attempts to overcome this difficulty have been made. In particular, indirect identification is a popular approach to mitigate this difficulty. Traditional indirect identification is a two-step procedure where the identification of a plant object is first obtained and then the open-loop system is unraveled from this preliminary estimate. Here, and in the sequel, we use the term "plant object" to refer to a transfer function that depends on the system. In traditional indirect identification, the plant object to be identified is usually the complementary sensitivity transfer function relating the reference signal to the output [5]. However, several difficulties are known to exist with this approach. For example, it is common that the identified open loop process is not necessarily stabilized by the controller used in the identification experiment, even though it is known that the real system is stabilized by this controller.

The objective of this paper is to find an open-loop model of a process using closed-loop data that has sufficient excitation exerted from the set-point and then design a robust controller to attain robustness against both model/parametric uncertainties and the effect of

external disturbances. Extending on [3], this paper investigates further the robustness of control with respect to mixed sensitivity based $\mathcal{H}_\infty$ control, and high order sliding mode control. It this regard, it aims to explore whether normal operating closed-loop data of a real process can be practically used to identify the open-loop process model and use these data to find the tuning parameters automatically. Hence, the objectives of our study here are as follows. Firstly, to be able to use normal operating closed loop data to model the open-loop process. Secondly, to identify the tuning parameters using famous tuning techniques. Thirdly, to develop linear and nonlinear robust controllers for the identified model to make the model robust in practice. An evaluation of the proposed scheme was performed on a benchmark laboratory-scale process control system using National Instruments LABVIEW. The paper is organized as follows. In Section 2, the process control system under study is described. Section 3 describes the system model and description. Section 4 deals with the evaluation of the proposed schemes on the physical system and Section 5 contains the conclusion.

2. The Proposed Scheme

The closed loop identification of a nonlinear system is proposed by the following stages developed, in order to find the correct model of the system as shown in Fig. 1. In the first stage, data-pretreatment is done in order to flush out the bias and outliers. In the second stage, excitation test is made for assuring the order of the model for the system. In the third stage, we find the process delay of the system. In the fourth stage, we find the process model followed by the fifth stage which involves the verification of accuracy of model. In the sixth stage, we find tuning constants, followed by the seventh stage, which involves finding the step response of the identified model

3. System Model and Description

The proposed scheme has been evaluated on a bench-marked laboratory scale two-tank apparatus, see Fig. 2. It is the most used prototype applied in waste water treatment, petrochemical, and oil/gas plants.

3.1. System Description

The bench-marked laboratory-scale process control system has been used to collect data. The data has been collected at a sampling time of 50 millisecond. The different data sets have been generated for PI control-based water level control. Different fault scenarios have also been considered for the generation of the data sets.

3.2. Experimental Setup

Process data has been generated through an experimental setup as shown in Fig. 3. A two tank system has been used in order to collect the data with the introduction of actuator, and sensor faults through the system as can be seen in the LABVIEW circuit window. An amplified voltage of 18 volts has been used to handle the controller effectively for the

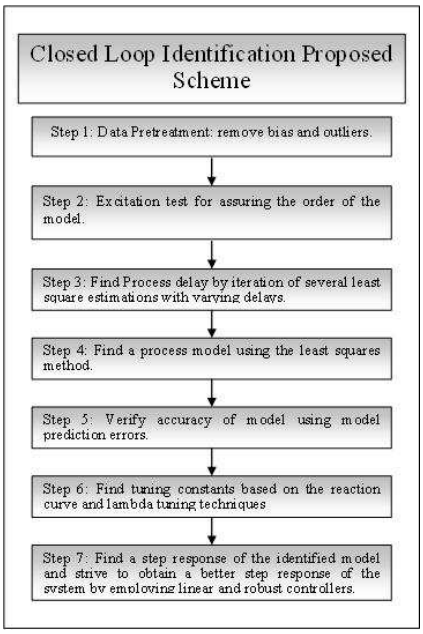

Figure 1. The Proposed scheme

changes/fluctuation produced in the system. So, the fault diagnosis was done over here in a closed loop identification where in the same time, the controller is suppressing the faults.

3.3. Process Data Collection and Description

The process data has been collected at 50 milli-seconds sampling time. The main objective of the bench-marked dual-tank system is to reach a reference height of 200 ml of the second tank. During this process, several faults have been introduced such as the leakage faults, sensor faults and actuator faults. Leakage faults have been introduced through the pipe clogs of the system, knobs between the first and the second tank etc. Sensor faults have been introduced by introducing a gain in the circuit as if there is a fault in the level sensor of the tank. Actuator faults have been introduced by introducing a gain in the setup for the actuator that comprises of the motor and pump. A PI controller has been employed in order to reach the desired reference height. Due to the inclusion of faults, the controller was finding it difficult to reach the desired level. For this reason, the power of the motor has been increased from 5 volts to 18 volts in order to provide it the maximum throttle to reach the desired level. In doing so, the actuator performed well in achieving its desired level but it also suppressed the faults of the system. So, it made the task of detecting the faults. After the collection of data, techniques such as settling time, steady state value, and coherence spectra can help us to give an insight of the fault.

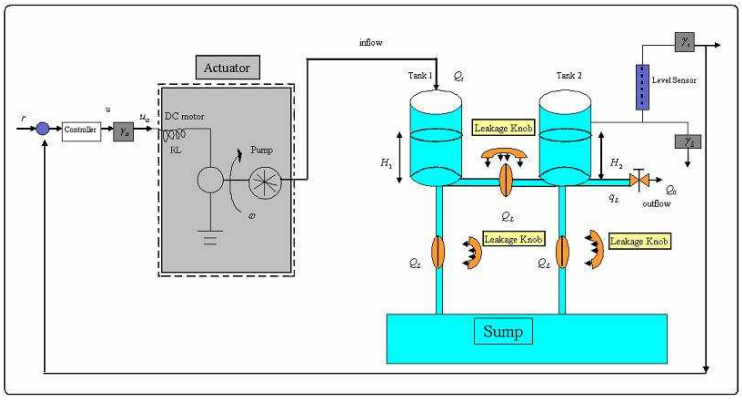

Figure 2. Two-tank fluid control system

3.4. Model of the Coupled Tank System

The physical system under evaluation is formed of two tanks connected by a pipe. The leakage is simulated in the tank by opening the drain valve. A DC motor-driven pump supplies the fluid to the first tank and a PI controller is used to control the fluid level in the second tank by maintaining the level at a specified level, as shown in Fig. 3. A step input is applied to the dc motor- pump system to fill the first tank. The opening of the drainage valve introduces a leakage in the tank. Various types of leakage faults are introduced and the liquid height in the second tank, H_2, and the inflow rate, Q_i, are both measured. The National Instruments LABVIEW package is employed to collect these data.

A benchmark model of a cascade connection of a dc motor and a pump relating the input to the motor, *u,* and the flow, Q_i, is a first-order system:

$$\dot{Q}_i = -a_m Q_i + b_m \phi(u) \tag{1}$$

where a_m and b_m are the parameters of the motor-pump system and $\phi(u)$ is a dead-band and saturation type of nonlinearity. It is assumed that the leakage Q_ℓ occurs in tank 1 and is given by:

$$Q_\ell = C_{d\ell}\sqrt{2gH_1} \tag{2}$$

With the inclusion of the leakage, the liquid level system is modeled by:

$$A_1 \frac{dH_1}{dt} = Q_i - C_{12}\varphi\left(H_1 - H_2\right) - C_\ell \varphi\left(H_1\right) \tag{3}$$

$$A_2 \frac{dH_2}{dt} = C_{12}\varphi\left(H_1 - H_2\right) - C_0 \varphi\left(H_2\right) \tag{4}$$

where $\varphi(.) = sign(.)\sqrt{2g(.)}$, $Q_\ell = C_\ell \varphi\left(H_1\right)$ is the leakage flow rate, $Q_0 = C_0 \varphi\left(H_2\right)$ is the output flow rate, H_1 is the height of the liquid in tank 1, H_2 is the height of the liquid

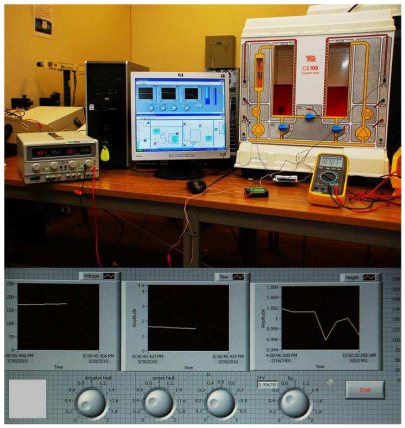

Figure 3. Top Figure: The two tank system interfaced with the Labview through a DAQ and the amplifier for the magnified voltage, Bottom Figure: The labview setup of the apparatus including the circuit window and the block diagram of the experiment.

in tank 2, A_1 and A_2 are the cross-sectional areas of the 2 tanks, $g = 980\ cm/\sec^2$ is the gravitational constant, C_{12} and C_0 are the discharge coefficient of the inter-tank and output valves, respectively.

The model of the two-tank fluid control system, shown above in Fig. 3 is of a second order and is nonlinear with a smooth square-root type of nonlinearity. For design purposes, a linearized model of the fluid system is required and is given below in (5) and (6):

$$\frac{dh_1}{dt} = b_1 q_i - (a_1 + \alpha)\, h_1 + a_1 h_2 \tag{5}$$

$$\frac{dh_2}{dt} = a_2 h_1 - (a_2 - \beta)\, h_2 \tag{6}$$

where h_1 and h_2 are the increments in the nominal (leakage-free) heights H_1^0 and H_2^0:

$$b_1 = \frac{1}{A_1}, \quad a_1 = \frac{C_{db}}{2\sqrt{2g(H_1^0 - H_2^0)}}, \quad \beta = \frac{C_0}{2\sqrt{2gH_2^0}},$$
$$a_2 = a_1 + \frac{C_{do}}{2\sqrt{2gH_2^0}} \quad \alpha = \frac{C_{d\ell}}{2\sqrt{2gH_1^0}}$$

and the parameter α indicates the amount of leakage.

A PI controller, with gains k_p and k_I, is used to maintain the level of the tank 2 at the desired reference input r as:

$$\begin{aligned} \dot{x}_3 &= e = r - h_2 \\ u &= k_p e + k_I x_3 \end{aligned} \tag{7}$$

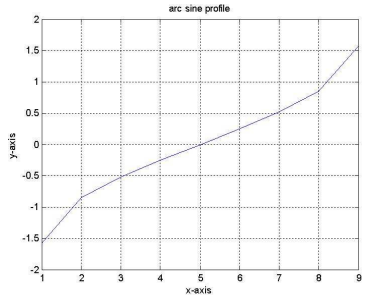

Figure 4. Sign(.) profile

The linearized model of the entire system formed by the motor, pump, and the tanks is given by:

$$\dot{x} = Ax + Br \quad y = Cx \tag{8}$$

where

$$x = \begin{bmatrix} h_1 \\ h_2 \\ x_3 \\ q_i \end{bmatrix}, \quad A = \begin{bmatrix} -a_1 - \alpha & a_1 & 0 & b_1 \\ a_2 & -a_2 - \beta & 0 & 0 \\ -1 & 0 & 0 & 0 \\ -b_m k_p & 0 & b_m k_I & -a_m \end{bmatrix}, \tag{9}$$

$$B = \begin{bmatrix} 0 & 0 & 1 & b_m k_p \end{bmatrix}^T, \quad C = [1 \quad 0 \quad 0 \quad 0]$$

where q_i, q_ℓ, q_0, h_1 and h_2 are the increments in Q_i, Q_ℓ, Q_0, H_1^0 and H_2^0, respectively, the parameters a_1 and a_2 are associated with linearization whereas the parameters α and β are respectively associated with the leakage and the output flow rate, i.e. $q_\ell = \alpha h_1$, $q_o = \beta h_2$.

Proposition: During the implementation process, sign(.) can be approximated with arc tangent. A relationship for approximation can be as follows:

$$sign(x) = \arctan(\frac{x}{\sqrt{1 - x * x}}), \ where \ x < 1$$

Likewise, after approximation, the profiles can be as follows. (See Figs. 4 and 5 where Fig. 4 representing the sign(.) profile and Fig. 5 representing the arctangent profile for a certain set of numbers are presented, respectively.)

4. Evaluation on a Physical System

The physical system under evaluation is formed of two tanks connected by a pipe. The leakage is simulated in the tank by opening the drain valve. A DC motor-driven pump

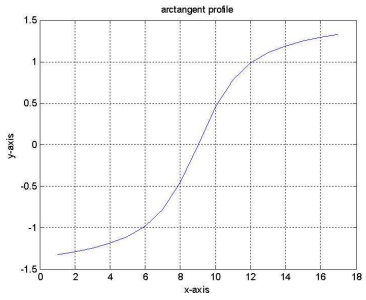

Figure 5. Arctangent profile for a certain set of numbers

supplies the fluid to the first tank and a PI controller is used to control the fluid level in the second tank by maintaining the level at a specified level, as shown in Fig. 2.

A step input is applied to the dc motor- pump system to fill the first tank. The opening of the drainage valve introduces a leakage in the tank. Various types of leakage faults are introduced and the liquid height in the second tank, and the inflow rate, are both measured. The National Instruments LABVIEW package is employed to collect these data. As mentioned earlier, various types of leakages were introduced by opening the drainage valve and the liquid height profiles in the second tank were subsequently analyzed.

4.1. Data pretreatment: removal of bias and outliers

The input/output data of a flow controller of a real process was collected at a rate of 1 sample per second to be used for this project. A graph showing, from top to bottom, the process output $y(t)$, the controller output $u(t)$ and the input reference signal $r(t)$ respectively (See Fig. 6).

A total of 5000 samples were collected from this process. Flow is measured using differential pressure measurement across an orifice plate with flange tapings. The controller used is a PI feedback controller with a controller gain of 0.15 which is measured by percent of full range of process output measurement over the full scale percentage of the controller output which is 100%. The integral constant T_i was 0.5 minute per repeat.

The data is already filtered at the transmitter device stage using a second-order filter with damping constant of 0.4 to filter out any high frequency noise. Hence, no further noise filtering of the data is necessary. The data pretreatment process for this project is designed to remove any outliers from the measurements. This is being shown in the following sections.

4.2. Persistent excitation test

The persistent excitation condition is the minimum requirement imposed on the test signal to guarantee that the estimation algorithms have unique solutions. For a finite impulse response model, the persistency-of-excitation test is found from the input correlation matrix

as follows:

$$R_{uu} = \begin{bmatrix} r_{uu}(0) & r_{uu}(1) & r_{uu}(2) & ... & r_{uu}(p-1) \\ r_{uu}(1) & r_{uu}(0) & r_{uu}(1) & ... & r_{uu}(p-2) \\ r_{uu}(2) & r_{uu}(1) & r_{uu}(0) & ... & r_{uu}(p-3) \\ .... & .... & .... & .... & .... \\ r_{uu}(p-1) & r_{uu}(p-2) & ... & ... & r_{uu}(0) \end{bmatrix} \tag{10}$$

Here, our objective is to find the maximum model order that can be found with reasonable accuracy. The degree of excitation of the input signal is defined as the order of a model that the input is capable of estimating in an unambiguous way. The process will do the following:

1. Find the correlation matrix of different sizes.

2. Determines the maximum matrix size by finding the singular values of the correlation matrices using a threshold of $1e^{-9}$.

3. If the technique determines that the maximum order is less than 5, the process will be terminated.

For the data provided, the result came out to be $n = 50$. Hence, the process will continue.

4.3. Finding the process delay

The process delay is found by an estimation which is based on a comparison of ARX models with different delays n_k.

$$\begin{aligned} &y(t) + a_1 y(t-1) + ... + a_{na} y(t-na) = b_1 u(t-nk) \\ &+ ... + b_{nb} u(t-nb-nk+1) \end{aligned} \tag{11}$$

The parameters are found using the least-squares method. The delay of the data used was found as 4 samples or 4 seconds. This is very reasonable for process control valves that have the speed of 0.15 inches per second for their stem movement.

4.4. Finding a process model using least squares method

The least-squares problem solution of a ARX model was found to be $\hat{\theta} = A^{\dagger} Y$, where $A^{\dagger}$ is the pseudo-inverse of the A given by:

$$A^{\dagger} = \left[A^T A\right]^{-1} A^T \tag{12}$$

where the minimization problem to be solved was:

$$\min_{\{\theta\}} \left\{ \left(Y(n) - A(n)\theta\right)^T \left(Y(n) - A(n)\theta\right) \right\}$$

The results were as follows:

DISCRETE TIME IDENTIFIED MODEL:

$$\begin{aligned} A(q)y(t) &= B(q)u(t) + e(t) \\ A(q) &= 1 - 0.7314q^{-1} + 0.01969q^{-2} - 0.06907q^{-3} \\ &\quad -0.1476q^{-4} \\ B(q) &= 0.1036q^{-4} - 0.0312q^{-5} - 0.03938q^{-6} \\ &\quad -0.02451q^{-7} \end{aligned} \tag{13}$$

SAMPLING INTERVAL $= 1$.

4.5. Finding the performance of the identified model

The commonly-used performance measures are unbiasedness, consistency and efficiency. Unbiasedness is guaranteed for ARX models because the noise is uncorrelated with the input data matrix. It measures the average value of the parameters and verifies that it is equal to the actual process parameter average.

The consistency involves the sum of squares of the residuals. One can validate the consistency of the identified model by verifying that:

$$E[res^T res] = (N - M)\sigma_v^2 \tag{14}$$

where N and M are the number of rows and columns of matrix A, respectively. Or, validation can be performed by taking the autocorrelation of the residuals, which should show that they are close to zero for all nonzero lags, that is, having a delta function-like shape.

The efficiency can be measured by finding the covariance of the model parameters from the real process parameters as $\mathrm{cov}(\bar{\theta}) = \sigma_v^2(A^T A)^{-1}$ The determinant of the covariance matrix of the prediction errors is the determinant of the noise variance matrix and it is called the Loss function (LossFcn). This value measures the prediction error reasonably well. It also provides the so called FPE: Akaike's Final Prediction Error (FPE), defined as the $LossFcn\ (1 + d/N)/(1 - d/N)$, where d is the number of estimated parameters and N is the length of the data record. The $LossFcn$ was used as a performance measure and it was found that $LossFcn = 0.000633849$ and $FPE = 0.000635884$. All performance tests show very good and reliable results for the identified model. Hence, we may proceed to the next step which is finding the tuning parameters of the controller. It should be noted that due to the presence of output feedback, the cross correlation between the input and the residuals showed negative values which is expected for feedback control loops as shown in Fig. 7.

4.6. Finding the tuning constants based on the reaction curve technique

The tuning constants can be found by using the reaction curve technique applied on the step response of the identified model found previously in step 6. The results of applying this technique and the comparison of the model approximation with the original step response model are shown in Figs 8 and 9 respectively.

Table 2. Ziegler Nocholas settings

CONTROLLER	KC	TI	TD
P	tau/(Kp $\times$ alpha)		
PI	0.9 $\times$ tau/(Kp $\times$ alpha)	3.33 $\times$ alpha	
PID	1.2 $\times$ tau/(Kp $\times$ alpha)	2 $\times$ alpha	0.5 $\times$ alpha

Table 3. Ziegler Nocholas settings

CONTROLLER	KC	TI	TD
P	2.4127		
PI	2.1715	13.32	
PID	2.8953	8	2

4.7. PID tuning

There are many PID tuning rules available for first-order plus time delay system models. The following tuning table was derived by Ziegler-Nichols to provide a quarter-decay ratio (the ratio of the second peak over the first peak) as shown in Table (2). Controller settings are shown in Table 3, where α is the time delay, τ is the time constant and K_P is the gain). The results were found as follows:

- Process gain: 0.120062,
- Time constant: 1.15871 sec,
- Time delay: 4 sec.

4.8. Step response of the identified model using PID

The step response model of the identified model is as shown below in Fig. 10. The open loop response of the system with leakage faults is as shown below in Fig. 11. The closed-loop step response has been simulated for the PID controller and is depicted in Fig. 12) which shows that the process output step response reaches the steady state after approximately 180 seconds or 3 minutes.

4.9. Step response of the identified model using $\mathcal{H}_\infty$ control

$\mathcal{H}_\infty$ controller has been often used for robust control of dynamical systems [16], [17], [18]. The aim of the $\mathcal{H}_\infty$ controller design is to track the reference input given by the operator and achieve the desired position in a minimum time and at a given performance level. For this purpose, we employed $\mathcal{H}_\infty$ controller for which the standard configuration is as shown in Fig. 13. The signals involved are: the control variable 'u', the measured variables 'v', the exogenous inputs 'w' such as disturbances and commands and the exogenous outputs

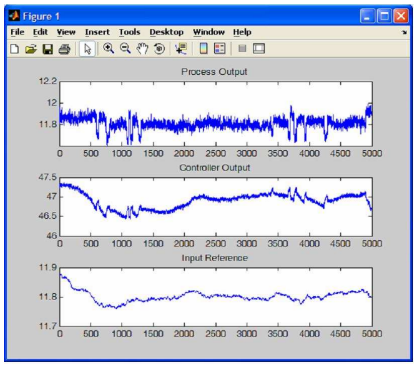

Figure 6. Process Output y(t), the controller output u(t), and Input reference signal r(t)

'z'. The closed-loop transfer function from w to z is given by the linear fractional transformation [16].

$$z = F_l(P, K)w \tag{15}$$

where $[F_l(P, K) = P_{11} + P_{12}K(I - P_{22}K)^{-1}P_{21}]$ standard $\mathcal{H}_\infty$ optimal control problem is to find all the stabilizing controllers K which minimize the following $\mathcal{H}_\infty$ norm:

$$\|F_l(P, K)\|_\infty = \max_\omega \bar{\sigma}(F_l(P, K)(j\omega)) \tag{16}$$

The $\mathcal{H}_\infty$ norm has several interpretations in terms of performance [16] where it minimizes the peak of the maximum singular value of $F_l(P, K)$. The general algorithm used to compute the controller is based on the solution presented in [16].

$\mathcal{H}_\infty$ loop shaping [16] is essentially a two-stage design procedure. First, the open-loop plant is augmented by a pre and a post-compensator as shown in Fig. 14 to give a desired shape to the singular values of the open-loop frequency response. Then the resulting shaped plant is robustly stabilized with respect to co-prime factor uncertainty using $\mathcal{H}_\infty$ optimization. The employed weights allow us to modify the model dynamics with a view to improving its tracking by increasing the gains at lower frequencies and changing the slope at the cross-over frequency to '1' so as to improve the controller's robustness. The re-shaped model of the identified plant can be utilized for controller synthesis as described in [17]. The design procedure resulted in an $\mathcal{H}_\infty$ controller with $\gamma_{\min} = 1.2817$, which confirms that our designed controller based on the identified model is robust against both external disturbances and system uncertainties. However, if we evaluate the performance of the system with the designed controller, we can observe that the system attains the desired level in less that 10 sec. which is much better than the results obtained with a PID controller. The step response in Fig. 15 shows that there is an overshoot in the system response and a small percentage of steady-state error.

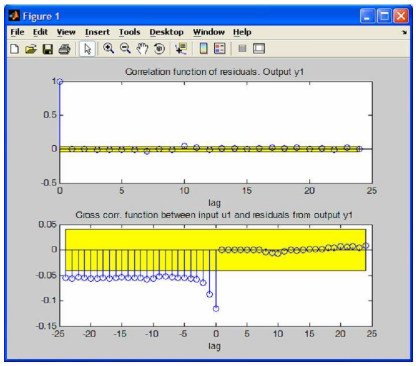

Figure 7. Cross correlation function between input u_1 and output y_1

4.10. Mixed Sensitivity Design

The closed-loop configuration [16] shown in Fig 16 in which d is the disturbance, n is the noise in the measurement sensors and r is reference input. In order to impose performance and robustness conditions the following closed-loop relationships between the output, the error, the control signal and the generalized disturbances acting on the system must be all taken in account:

$$\begin{aligned} y &= T_o r + S_o d - T_o n \\ e &= S_o(r-d) + T_o n \\ u &= K S_o(r-n-d) \end{aligned} \tag{17}$$

In the above expression the $W_s(.)$ and $W_u(.)$ are the weighting functions, which are employed to shape the closed-loop transfer function S_o and T_o respectively. Fig. 17 shows the new augmented plant configuration and Fig. 18 indicates the step response of the design.

Therefore, shaping T_o is desirable for tracking problems, noise attenuation and robust stability with respect to multiplicative uncertainty. On the other hand, shaping will allow the control of the system's performance. In addition the control signal should be attenuated along the frequency.

The resolution may be carried out by means of mixed sensitivity problem S/KS [16]. The optimal control is formulated as finding a stabilizing controller K(s) such that the following expression is minimized.

$$\min_{k(s)} \left\| \begin{bmatrix} W_s(s)S_o(s) \\ W_u(s)K(s)S_o(s) \end{bmatrix} \right\|_\infty \tag{18}$$

4.11. Step response of the identified model using sliding mode control

As an alternative robust controller, a sliding mode controller has been designed for the identified model. In sliding-mode control design, a hyper-plane is defined as a sliding

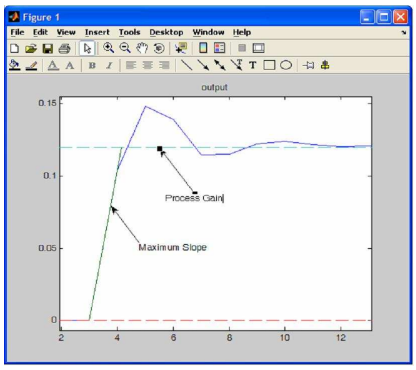

Figure 8. Reaction curve technique

surface. This design approach comprises of two stages: the first one is the reaching phase and the second one is the sliding phase. In the reaching phase, the system's states are driven to a stable manifold by the help of an appropriate equivalent control law and in the sliding phase, these states slide to an equilibrium point. One advantage of this design approach is that the effect of nonlinear terms, which may be construed as a disturbance or as an uncertainty in the nominal plant, have been completely rejected. Another benefit accruing from this situation is that the system is forced to behave as a reduced order system; this guarantees the absence of overshoot while attempting to regulate the system from an arbitrary initial condition to the designed equilibrium point. The design of a sliding-mode controller for the identified model is carried out by defining the sliding manifold based on its error dynamics defined as [19]:

$$e = x - x_d \tag{19}$$

where x_d is the desired value of the system state at the equilibrium position. For the above-discussed design approach, the sliding manifolds are designed as follows:

$$S = e_1 \tag{20}$$

The system error tends to zero if $S = 0$ and the rate of convergence will be governed by the manifold dynamics. The Lyapunov function [20], for the surfaces defined above can be written as:

$$V = \frac{1}{2}s^2, \tag{21}$$

which are positive-definite functions and their time derivative can be written as:

$$\dot{V} = s\dot{s} \tag{22}$$

The equivalent control u_{eq} on the manifold $s_1 = e_1 = 0$ can be shown to be equal to:

$$u_{eq} = \frac{0.04276}{0.0625}x_1 \tag{23}$$

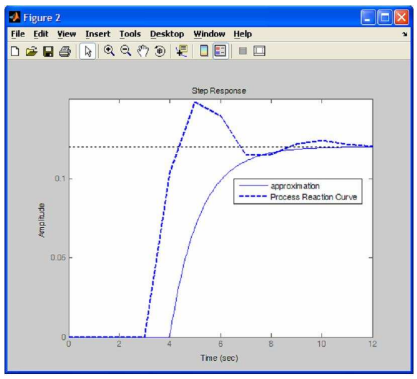

Figure 9. Comparison of model approximation and the original step response model

The control input vector 'u' that will make the system converge at $S = 0$ can be written as:

$$u = u_{eq} - Ksign(s) \tag{24}$$

This control law will ensure both the system's convergence to a sliding manifold and robustness against the system uncertainties and external disturbances. To avoid high frequency switching, i.e. chattering, implementation of the control laws have been performed by employing a saturation function [19] defined as:

$$sat(s) = sign(\frac{s}{\varepsilon}); \quad if \quad abs(\frac{s}{\varepsilon}) > 1$$
$$sat(s) = \frac{s}{\varepsilon} : \quad if \quad abs(\frac{s}{\varepsilon}) < 1$$

The chattering reduction depends on the value of ϵ in the range $\epsilon < 1$ but at the cost of robustness. The higher the value of , the lesser the chattering will be and the more reduced the robustness will be too. Now by substituting the defined control laws in equation (12), we get:

$$\dot{V} = -s^2 \tag{25}$$

$\dot{V}$ will always be negative-definite for non-zero manifolds.

In the first phase of controller validation, only simulations are carried out. But later, the designed controller was tested on real data extracted from a physical two-tank system, and it delivered the desired tracking control of the identified model as shown in Fig. 19 along with sliding manifolds convergence. The convergence of states is in finite time with no overshoot and steady state error. The robust nature of sliding mode control makes the identified system indifferent to parametric uncertainties and external disturbances. However the performance of the system is best in the previously discussed and simulated controllers, that is, the system reaches the desired level in less than 6 seconds which is almost twice as fast as its linear counter part.

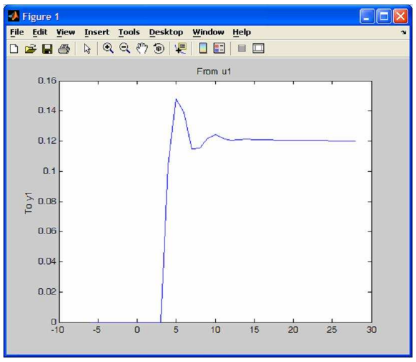

Figure 10. Step response of the identified model

4.12. Higher Order Sliding Mode Control (HOSM)

HOSM [21], [22], [23] is a recent approach that allows the removal of all standard sliding mode restrictions, while preserving the main sliding mode feature and improving its accuracy. Traditional SMC has some intrinsic problems, such as discontinuous control that often yields chattering [20]. To cope with this problem and achieve a higher accuracy, HOSM is proposed [21], [22]. Obviously, a k^{th} order HOSM stabilizes the sliding variable at zero as well as its k-1 derivatives to zero. On the other hand, since the high-frequency switching is hidden in the higher derivative of the sliding variable, the effect of chattering will be inherently reduced. In other words, HOSM has two important features that make it a better choice in designing the desired controller. It improves the accuracy of the design, which is a very important issue, and may provide a continuous control. See the step response with second order sliding mode control in Fig. 20.

The super twisting continuous control law [23] consists of two terms. The first term is defined by means of its discontinuous time derivatives, while the other is a continuous function of the available sliding variable. Consider the control algorithm

$$u_i(t) = u_i^{'}(t) + u_i^{''}(t) i = 1, 2 \tag{26}$$

$$u_i^{'}(t) = -\alpha_i |\sigma_i|^p sign(\sigma_i) i = 1, 2 \tag{27}$$

where

$$\dot{u}_i^{''}(t) = \begin{cases} -u_i(t) & \text{if } |u_i| > 1 \\ -\beta_i sign(\sigma)_i & \text{if} |u_i| \leq 1 \end{cases} \tag{28}$$

The values of the constants (α_1, β_i) values [23] are computed while keeping in mind the following bounds defined as:

$$\begin{cases} \alpha_i > \frac{\Phi_i}{\Gamma_{m_i}} \\ \beta_i^2 \geq \frac{4\Phi_i}{\Gamma_{m_i}^2} \frac{\Gamma_{M_i}(\alpha_i + \Phi_i)}{\Gamma_{M_i}(\alpha_i - \Phi_i)} \\ 0 < \rho \leq 0.5 \end{cases} \tag{29}$$

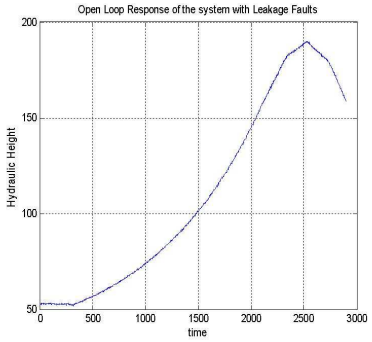

Figure 11. Open loop response of the system with leakage faults

5. Conclusions

In this paper, a new scheme for closed loop identification has been developed and successfully tested on a two-tank system. It has been shown that it is possible to model a process while the controller is in an open-loop setting. The developed process model has been incorporated in the design of robust controllers. The designed robust controllers have been shown to outperform the traditional controllers of single-term (P), two-terms (PI) and three-terms (PID) and guarantee the desired performance of the system along with robustness against parametric and model uncertainties as well as the effects of external disturbances. This work also provides ample encouragement to be applied and extended to other industrial process control systems, such as three-tank systems, distillation columns, to name a few.

Acknowledgment

The authors wish to acknowledge the support by the deanship of scientific research (DSR) at KFUPM through the research project No. **IN100018**.

References

[1] Forssell, U., and Ljung, L., 'Closed loop identification revisited', *Automatica*, 1999, vol. 35, pp. 1215–1241.

[2] Goodwin, G., and Payne, R., *Dynamic system identification: Experiment design and data analysis*, Academic Press, 1977.

[3] Doraiswami, R., Cheded, L., Khalid, H. M., Ahmed, Q., and Khoukhi, A., 'Robust Control of a Closed loop identified system with parametric/model uncertainties and external disturbances', *International Conference on Systems, Modeling and Simulations*, January 27-29, 2010, Liverpool, UK, pp. 270–275.

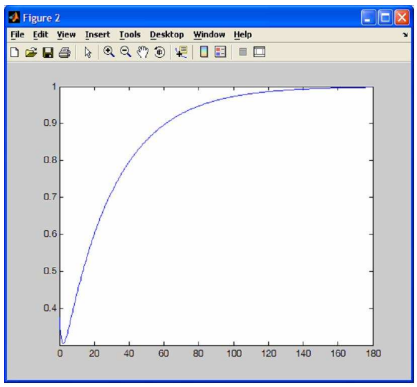

Figure 12. Closed loop response for PID controller

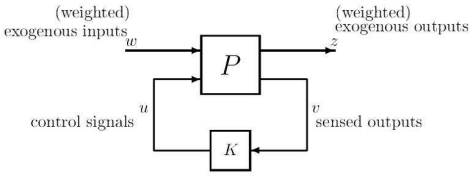

Figure 13. General control configuration for $\mathcal{H}_\infty$ control

[4] Ljung, L., 'System Identification: Theory for the user', Prentice Hall, 1999, 2nd edition.

[5] Soderstrom, T., and Stoica, P., 'System identification', *Prentice-Hall*, 1989.

[6] Van den Hof, P., 'Closed-loop issues in system identification', *Annual Reviews in Control*, vol. 22, 1998, pp. 173–186.

[7] Gevers, M., 'Identification for control: from the early achievements to the revival of experiment design', *European Journal of Control*, 2005, vol. 11, no. 4-5, pp. 335–352.

[8] Hjalmarsson, H., 'From experiment design to closed-loop control', *Automatica*, vol. 41(3), 2005. pp. 393–438.

[9] Hjalmarsson, H., Gevers, M., and De Bruyne, F., 'For model-based control design, closed-loop identification gives better performance', *Automatica*, vol. 32(12), 11996, pp. 1659–1673.

[10] Van den Hof, P., and Schrama, R., 'Identification and control closed loop issues', *Automatica*, vol. 31(12), 1995, pp. 1751–1770.

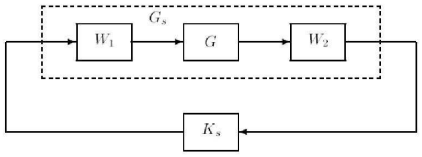

Figure 14. Loop shaping design procedure implementation

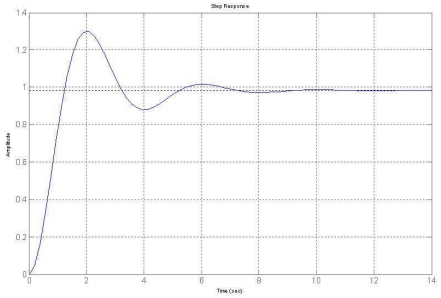

Figure 15. Step response of the identified model using $\mathcal{H}_\infty$ control

[11] Aguero, J., and Goodwin, G., 'Choosing between open and closed-loop experiments in linear system identification', *IEEE Trans. Automatic Control*, 2007, vol. 52(8), pp. 1475–1480.

[12] Bavdekar, V. A., Anjali P. Deshpande and Sachin C. Patwardhan, 'Identification of process and measurement noise covariance for state and parameter estimation using extended Kalman filter', *J. Process Control*, vol. 21(4), pp. 585–601, 2011.

[13] Romano, R. A. and Claudio Garcia, 'Valve friction and nonlinear process model closed-loop identification', *J. Process Control*, vol. 21(4), pp. 652–666, 2011.

[14] Badwe, A. S., Sachin C. Patwardhan, Ravindra D. Gudi, 'Closed-loop identification using direct approach and high order ARX/GOBF-ARX models', *Journal of Process Control*, vol. 21(7), pp. 1056–1071, 2011.

[15] Yuri A., W. Shardt and Biao Huang, 'Closed-loop identification with routine operating data: Effect of time delay and sampling time', *J. Process Control*, vol. 21(7), pp. 997–1010, 2011.

[16] Skogestad, S., and Postlethwaite, I., 'Multivariable feedback control, analysis and design', *John Wiley & Sons*, New York.

[17] Doyle, J.Grover, K.Khargonekar, and Francis, B., 'State space solutions to standard $\mathcal{H}_2$ and $\mathcal{H}_\infty$ control problems', *IEEE Trans. Automatic control*, vol. 34(8), pp. 831–846, August 1989.

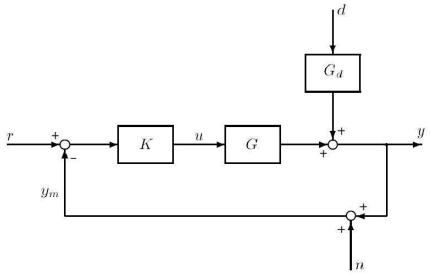

Figure 16. Closed loop system

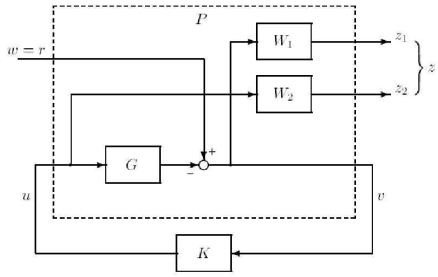

Figure 17. Augmented plant configuration

[18] Ahmed, Q., Bhatti, A., Iqbal, S., 'Robust decoupling control design for twin rotor system using hadamard weights', *Proc. of CCA*, MSC 2009, St. Petersburg, Russia, pp. 1009–1014.

[19] Ahmed, Q., Bhatti, A., Iqbal, S., 'Nonlinear robust decoupling control design for twin rotor system', *Proc. Asian Control Conference* 2009, Hong Kong.

[20] Slotine, J., Li, W., *Applied nonlinear control*, Prentice Hall, 1991.

[21] Levant, A., 'Universal SISO sliding mode controllers with finite-time convergence', *IEEE Transactions on Automatic Control*, vol. 46(9), 1998, pp. 1447–1451.

[22] Emelyanove, S., Korovin, S., and Levant, A., 'Higher-order sliding modes in control systems', *Differential Equations*, vol. 29, 1993, pp. 1627–1647.

[23] Perruquetti, W., Dekker, M., *Sliding mode control in engineering*, Inc., 2002.

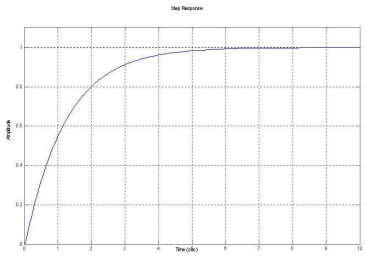

Figure 18. Step response with mixed sensitivity based $\mathcal{H}_\infty$ controller

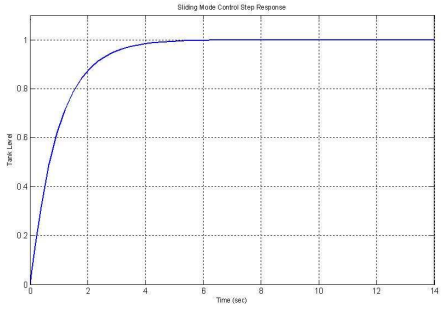

Figure 19. Step response of the identified model using sliding mode control

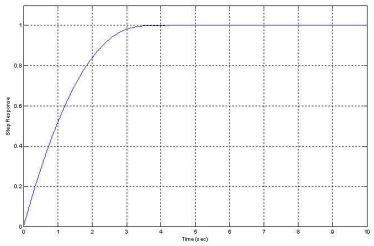

Figure 20. Step response with second order sliding mode control